

# Discovery of a widely separated ultracool dwarf – white dwarf binary

A. C. Day-Jones<sup>1\*</sup>, D. J. Pinfield<sup>1</sup>, R. Napiwotzki<sup>1</sup>, B. Burningham<sup>1</sup>, J. S. Jenkins<sup>1,2</sup>,

H. R. A. Jones<sup>1</sup>, S. L. Folkes<sup>1</sup>, D. J. Weights<sup>1</sup> and J. R. A. Clarke<sup>1</sup>

<sup>1</sup> *Centre for Astrophysics Research, University of Hertfordshire, College Lane, Hatfield, Hertfordshire, AL10 9AB, UK*

<sup>2</sup> *Penn State University, State College, PA 16802, U.S.*

## ABSTRACT

We present the discovery of the widest known ultracool dwarf – white dwarf binary. This binary is the first spectroscopically confirmed widely separated system from our target sample. We have used the 2MASS and SuperCOSMOS archives in the southern hemisphere, searching for very widely separated ultracool dwarf – white dwarf binaries, and find one common proper motion system, with a separation of 3650 – 5250 AU at an estimated distance of 41 – 59 pc, making it the widest known system of this type. Spectroscopy reveals 2MASS J0030 – 3740 is a DA white dwarf with  $T_{\text{eff}}=7600 \pm 100\text{K}$ ,  $\log(g)=7.79 - 8.09$  and  $M_{WD} = 0.48 - 0.65 M_{\odot}$ . We spectroscopically type the ultracool dwarf companion (2MASS J0030 – 3739) as  $M9 \pm 1$  and estimate a mass of  $0.07 - 0.08 M_{\odot}$ ,  $T_{\text{eff}} = 2000 - 2400 \text{K}$  and  $\log(g)=5.30 - 5.35$ , placing it near the mass limit for brown dwarfs. We estimate the age of the system to be  $>1.94$  Gyrs (from the white dwarf cooling age and the likely length of the main sequence lifetime of the progenitor) and suggest that this system and other such wide binaries can be used as benchmark ultracool dwarfs.

**Key words:** Stars: low mass, brown dwarfs - stars: white dwarfs - binaries: general

## 1 INTRODUCTION

The rise of deep large area surveys such as 2MASS (the Two Micron All Sky Survey), SDSS (the Sloan Digital Sky Survey) and UKIDSS (the UK Infrared Deep Sky Survey) has increased the number of known brown dwarfs to several hundred, since the discovery of Gliese 229B (Nakajima et al. 1995) and Tiede 1 (Rebolo et al. 1995) just over a decade ago. These populations have helped shape our understanding of ultracool dwarfs (UCDs; with spectral type  $\geq M7$  e.g. Jones & Steele 2001) and revolutionized the classification system for sub-stellar objects including the creation of two new spectral types L and T. The latest M dwarfs ( $\sim M7-9$ ) have effective temperature ( $T_{\text{eff}}$ ) reaching down to  $\sim 2300\text{K}$ . At lower  $T_{\text{eff}}$  ( $\sim 2300-1400 \text{K}$ ) are the L dwarfs, which have very dusty upper atmospheres and generally very red colours. T dwarfs are even cooler having  $T_{\text{eff}}$  in the range  $\sim 1400-650 \text{K}$ , where the low  $T_{\text{eff}}$  limit is currently defined by the recently discovered T8+ dwarfs, ULAS J0034-0052 (Warren et al. 2007) and CFBD5 J005910.90-011401.3

(Delorme et al. 2008). T dwarf spectra are dominated by strong water vapour and methane bands, and generally appear very blue in the near infrared (Geballe et al. 2003; Burgasser et al. 2006).

The physics of ultracool atmospheres is complex, and very difficult to accurately model. Atmospheric dust formation is particularly challenging for theory (Allard et al. 2001; Burrows, Sudarsky & Hubeny 2006), and there are a variety of other important issues that are not well understood, including the completeness of  $\text{CH}_4/\text{H}_2\text{O}$  molecular opacities, their dependence on  $T_{\text{eff}}$ , gravity and metallicity (e.g. Jones et al. 2005; Burgasser et al. 2006a; Liu, Leggett & Chui 2007), as well as the possible presence of vertical mixing in such atmospheres (Saumon et al. 2007). The emergent spectra from ultracool atmospheres are strongly affected by factors such as gravity and metallicity (e.g. Knapp et al. 2004; Burgasser et al. 2006a; Metchev & Hillenbrand 2006), and we must improve our understanding of such effects if we are to be able to spectroscopically constrain atmospheric and physical properties (such as mass, age and composition) of low-mass/sub-stellar field populations.

Discovering UCDs whose properties can be inferred indirectly (without the need for atmospheric models) is an

\* E-mail: a.c.day-jones@herts.ac.uk. Based on observations made with ESO telescopes at the La Silla Paranal Observatory under programme 278.C-5024(A)

excellent way to provide a test-bed for theory, and observationally pin down how physical properties affect spectra. We refer to such UCDs as *benchmark* objects (e.g. Pinfield et al. 2006). A population of benchmark UCDs with a broad range of atmospheric properties will be invaluable in the task of determining the full extent of spectral sensitivity to variations in UCD physical properties. However, such benchmarks are not common, and the constraints on their properties are not always particularly strong.

One variety of benchmark UCD that could yield accurate ages and surface gravities over a broad age range are in binary systems with a white dwarf (WD) companion. In particular, if the WD is relatively high mass, then the main sequence progenitor star will have a short lifetime, and the age of the binary system (and the UCD) will essentially be the same as the cooling age of the WD, which can be well determined from theory.

There have been several searches to find UCD companions to WDs. Despite this, only a small number of detached UCD–WD binaries have been identified; GD 165B(L4) (Zuckerman & Becklin 1992), GD 1400(L6/7) (Farihi & Christopher 2004; Dobbie et al. 2005), WD 0137 – 349(L8) (Maxted et al. 2006; Burleigh et al. 2006) and PG1234+482 (L0) (Steele et al. 2007; Mullally et al. 2007). The two components in GD 165 are separated by 120 AU, the separation of the components in GD 1400 and PG 1234 + 482 are currently unknown and WD 0137 – 349 is a close binary (semi-major axis  $a = 0.65 R_{\odot}$ ). Farihi, Becklin & Zuckerman (2005) and Farihi, Hoard & Wachter (2006) also identified three late M companions to white dwarfs; WD2151 – 015 (M8 at 23 AU), WD2351 – 335 (M8 at 2054 AU) and WD1241 – 010 (M9 at 284 AU). The widest system previously known was an M8.5 dwarf in a triple system – a wide companion to the M4/WD binary LHS 4039 and LHS 4040 (Scholz et al. 2004), with a separation of 2200 AU. There are several other known UCD–WD binaries, however these are cataclysmic variables (e.g. SDSS 1035; Littlefair et al. 2006, SDSS1212; Burleigh et al. 2006, Farihi, Burleigh & Hoard 2008, EF Eri; Howell & Ciardi 2001) but these are unlikely to provide the type of information that will be useful as benchmarks, as they have either evolved to low masses via mass transfer or their ages cannot be determined because of previous evolutionary phases (e.g. common envelope). WD0137-349 is also not likely to be useful as a benchmark due to the large uncertainty in age caused by the common envelope stage and the heating from the white dwarf.

Recent analysis from Farihi, Becklin & Zuckerman (2008) shows that the fraction of brown dwarf companions (L and T) at separations within a few hundred AU of white dwarfs is <0.6 per cent. However, despite this UCDs in wide binary systems are not uncommon (revealed through common proper motion) around main sequence stars at separations of 1000 – 5000 AU (Gizis et al. 2001; Pinfield et al. 2006). However, when a star sheds its envelope post-main sequence, we may expect a UCD companion to migrate outwards to even wider separation (Jeans 1924; Burleigh, Clarke & Hodgkin 2002), and UCD–WD binaries could thus have separations up to a few tens of thousands of AU. Although some of the widest binaries may be dynamically broken apart quite rapidly by gravitational interactions

with neighbouring stars, some systems may survive, offering a significant repository of benchmark UCDs.

We present here the first results from our search of 2MASS and the digitized Schmidt plate archive SuperCOSMOS, for wide UCD–WD binaries in the southern sky, and present our first discovery of a wide UCD–WD binary confirmed through common proper motion and spectroscopy. In Section 2 we describe the techniques we have developed to select candidate UCD–WD binary systems using database photometry and proper motion. Section 3 describes our second epoch imaging of candidates, and followup infrared and optical spectroscopy along with proper motion analysis. We present spectroscopic analysis in Section 4. Section 5 discusses the newly discovered system, and Section 6 presents a discussion of future work.

## 2 CANDIDATE BINARY SELECTION

### 2.1 Selecting white dwarf candidates

Candidate WDs were selected from the SuperCOSMOS Science Archive (SSA), following a similar technique to that of Knox et al. (1999). We selected candidates based on their position on a reduced proper motion (RPM) diagram, a technique that uses proper motion as a distance proxy, taking advantage of the fact that nearby objects in general have higher proper motion. Fig. 1 shows our SuperCOSMOS RPM diagram. Our initial SSA sample (shown as dots) was a magnitude selected sample ( $R \leq 20$ ) to avoid sources near the plate limit. We also selected against non-moving sources (by requiring  $PM \geq 10 \text{ mas yr}^{-1}$ ,  $PM/\sigma_{PM} \geq 5$ ), and against non stellar sources (requiring a database star-like class=2). In addition we avoid the galactic plane (requiring  $|b| \geq 25^\circ$ ), require SSA *I*-band coverage ( $\delta \leq +3^\circ$ ; which offers possible additional epochs for nearby UCD candidates; see Section 3.3), and impose a quality constraint on the database photometry (qual $\leq 1040$  in each of the *B*-, *R*- and *I*-bands, indicating the the object is unlikely to be a bright star artifact.).

The main sequence and WD sequence can be clearly seen in Fig. 1, and display good separation for  $B - R \leq 1.3$ . To further illustrate the location of the WD sequence, we over plot the positions of WDs from the spectroscopically confirmed McCook & Sion WD catalogue (McCook & Sion 1999; here after MS99), along with pre-WDs (i.e. sdO stars) and Halo objects from Leggett (1992). We also overplot subdwarf B stars, hot, cool and extreme subdwarfs from Kilkenny, Heber & Drilling (1988), Stark & Wade (2003), Yong & Lambert (2003) and Monet et al. (1992) respectively. These, like halo objects can have high velocity dispersions and can masquerade as white dwarfs in RPM diagrams. The overplotted populations help confirm the location of the WD sequence for  $B - R \leq 1.3$ , and allow us to assess the location of WDs out to redder colour. Our final RPM selection criteria were chosen to strike the best balance between WD selection and contamination minimisation, and are shown in Fig. 1 as dashed lines. At the red end in particular, we have attempted to include as many WD candidates as possible, while avoiding contamination from cool subdwarfs.

The RPM selection criteria are

$$H_R \geq 8.9(B - R) + 10.5 \text{ for } B - R \leq 0.65 \text{ and}$$

**Table 1.** Galactic co-ordinates of contaminated and overcrowded regions removed from our selection.

Region	$l_{\min}$	$l_{\max}$	$b_{\min}$	$b_{\max}$
SMC.....	300°	310°	-42°	-23°
LMC.....	270°	290°	-40°	-25°
.....	145°	220°	-42°	-20°
.....	20°	45°	-25°	-20°

$$H_R \geq 4.1(B - R) + 12.5 \text{ for } B - R > 0.65;$$

Our selection criteria resulted in a sample of 1532 WD candidates.

## 2.2 Selecting ultracool dwarf candidates

UCD candidates were photometrically selected by their near infrared (NIR) colours from the 2MASS all sky point source catalogue, using the NASA/IPAC Gator search engine. We used colour cut criteria devised by Folkes et al. (2007), which are based on the colours of known L-dwarfs with reliable  $J$ -,  $H$ - and  $K$ - band 2MASS photometry ( $\text{SNR} \geq 20$ ) from the Caltech cool dwarf archive (DWARFARCHIVES.ORG), requiring the following photometric criteria to be met:

$$\begin{aligned} 0.5 &\leq J - H \leq 1.6 \\ 1.1 &\leq J - K \leq 2.8 \\ 0.4 &\leq H - K \leq 1.1 \\ J - H &\leq 1.75(H - K) + 0.37 \\ J - H &\geq 1.65(H - K) - 0.35 \\ \text{and } J &\leq 16.0. \end{aligned}$$

We also imposed an optical-NIR colour restriction using the USNO-A2.0 cross-match facility within the Gator, ruling out objects with  $R - K < 5.5$  ( $a = U$  combined with  $\text{vr\_m\_opt-}K > 5.5$ , or  $\text{nopt\_mchs}=0$ ). In addition certain sky coverage constraints were imposed, and we made use of the 2MASS data quality criteria and some additional database flags, to remove contamination from artefacts and low quality photometric data (requiring  $\text{cc\_flag}=000$ ,  $\text{ph\_qual} \leq \text{CCC}$ ,  $\text{jhk\_snr} > 5$ ,  $\text{gal\_contam}=0$ ,  $\text{prox} > 6$ ) and known contaminants ( $\text{mp\_flg}=0$ ). As with the WD candidate selection, we searched areas away from the galactic plane ( $|b| > 25^\circ$ ) to avoid confusion from over crowding and contamination from reddened stars and giants. We also avoided  $|\delta| > 86^\circ$ , for which 2MASS suffers from incompleteness issues with its optical cross-matching. Additional areas surrounding the Small and Large Magellanic clouds were also ignored. Finally two additional uncatalogued, reddened regions were avoided following the approach of Cruz et al. (2003). These excluded regions are listed in Table 1, and the resultant sky coverage of our survey is 13,216 sq. degs, or 32 per cent of the sky. Visual inspection of all these candidates (13,338 in number) was neither practical or necessary at this stage, and we thus postponed our visual inspection until after our binary pair selection procedure (see next Section).

## 2.3 Selection of candidate binary pairs

To identify very widely separated UCD-WD binary candidates, we searched for pairs with separations out to 20,000AU, allowing for an outward migration factor of  $\sim 4$

(during the post-main-sequence mass-loss phase) from the known separations of wide UCD – main-sequence star binaries (5,000AU; see Section 1). To illustrate this choice, consider a WD of mass  $\sim 0.65 M_\odot$  (the mean of the WD mass distribution). The progenitor mass would be  $\sim 2.7 M_\odot$  (from the initial-final mass relation from Dobbie et al. 2006) so  $M_{\text{initial}}/M_{\text{final}} \sim 4$  (Jeans 1924). We thus suggest that the projected maximum orbital separation could be up to  $\sim 20,000\text{AU}$ . In addition, we imposed the constraint that the photometry of any UCD and WD pairs associated as candidate binaries, be consistent with these objects being at the same distance. In order to do this, reasonable distance constraints were required for both types of object.

We started by placing a distance constraint on the WDs, by constructing an  $M_B$  against  $B - R$  colour magnitude diagram (CMD), using a combination of observed and theoretical WD photometry; this CMD is shown in Fig. 2. Known WDs were taken from MS99, including all WDs with known parallax and distance uncertainties better than 20 per cent. These objects are plotted as crosses with associated error bars. In addition synthetic WD properties (luminosity,  $T_{\text{eff}}$  and  $\log(g)$ ) were obtained for three different masses (0.5, 0.7 and  $1.2 M_\odot$ ) over a range of disk ages, using equations from Schröder, Pauli & Napiwotzki (2004), and the mass-radius relation of Panei, Althaus & Benvenuto (2000). Synthetic WD photometric properties were then determined using a combination of colour- $T_{\text{eff}}$  and  $\text{BC-}T_{\text{eff}}$  relations from models (Chabrier et al. 2000) and observation (Kleinmann et al. 2004). The photometry was transformed into the SuperCOSMOS system using relations given in Bessell. (1986). These theoretical tracks are shown in Fig. 2 as dotted, dashed, and dot-dash lines respectively.

We defined a WD region in the CMD (shown by the solid lines) to take into account the spread seen in both observation and the models, while also offering a reasonably constrained WD sequence (that will yield useful distance constraints). Although some of the hottest WD model tracks lie slightly above our region, we note that no such trend is seen for the observations, and that the highest mass hot model points are completely contained within it. This is desirable since high mass WDs are more interesting in the context of benchmark UCDs. Using this CMD as an aid for characterising WDs, we used the  $B - R$  colour for each of our WD candidates to estimate a possible range of  $M_B$ , thus derived a corresponding distance range appropriate to the measured  $B$ - magnitude of each candidate.

We then used the lower distance estimates to provide upper limits to the angular separation corresponding to 20,000AU at the distance of each of the WD candidates, and searched for UCD candidates whose angular separation from the WDs was within the appropriate limit. We also used the UCD colour-magnitude information to check for consistency between candidate binary pairs, by using the WD distance estimates to convert UCD candidate  $J$ - band magnitudes into  $M_J$ . This assumes that the two objects are at the same distance. We then plotted the UCD candidate on an  $M_J$  against  $J - K$  CMD, to see if it was located in the expected part of the diagram. Fig. 3 shows this NIR CMD, with the known location of previously confirmed UCDs (with parallax distances from Knapp et al. 2004). We defined a similar UCD CMD selection region as Pinfield et al. (2006), which is shown as a dashed line box. If UCD candidates lie out-

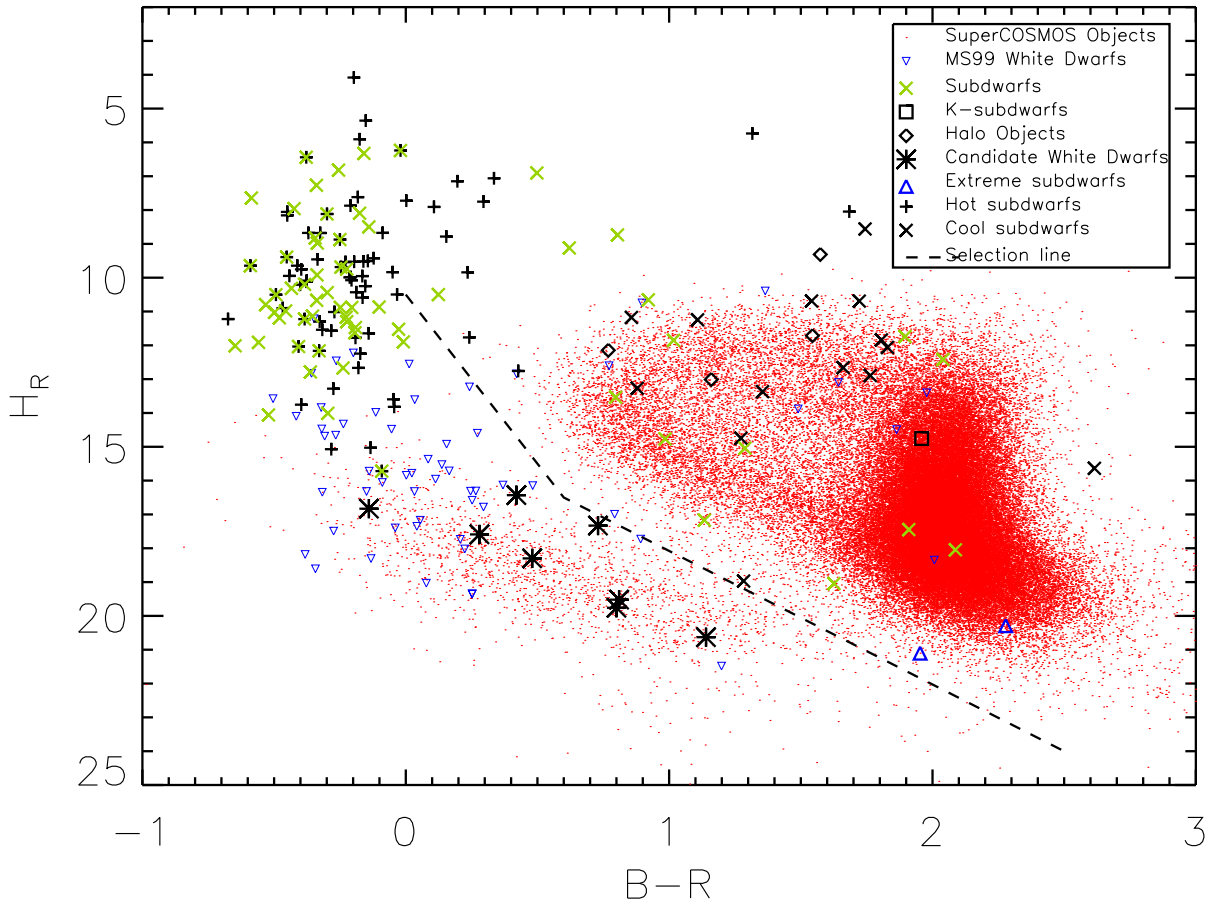


**Figure 1.** Reduced Proper Motion (RPM) diagram showing how WD candidates were selected from SuperCOSMOS. We chose candidate WDs from amongst our initial (see text) SuperCOSMOS sample (points) using a cut in colour-RPM space ( $RPM = H_R = R + 5 \log \mu + 5$ ), which is overplotted in the figure as a dashed line. Highlighted are spectroscopically confirmed WDs from MS99 (upside down triangles), hot subdwarfs (plus signs), cool subdwarfs (crosses) and extreme subdwarfs (triangles) to help delineate the WD sequence. The location of some halo objects (diamonds and squares) are also indicated. Also shown are the WD components of our eight candidate UCD – WD binaries (stars).

side this box, then their photometry is deemed inconsistent with a UCD at the same distance as the neighbouring candidate WD. All possible pairs were considered amongst our 1532 WD and 13,338 UCD candidates, and assessed with our separation and photometric consistency tests. In this way we identified 18 candidate UCD–WD binary systems. These candidates were visually inspected using images from 2MASS, SuperCOSMOS and DENIS (where available). We find that seven of the UCD candidates have bright  $R$ -band counterparts and were therefore rejected as their  $R-J$  colour is too blue. Proper motion analysis using  $I$ -band schmidt plates from SuperCOSMOS and 2MASS  $J$ -band images revealed that three are non common proper motion. The UCD and WD components from the eight remaining candidate pairs are presented in Table 2 and over-plotted as stars in Fig. 1 and 3. The clumping in to the top left of the selection space in Fig. 3 reflects our greater sensitivity to closer, brighter late M and L dwarfs in 2MASS.

### 3 FOLLOWUP OBSERVATIONS & DATA REDUCTION

#### 3.1 Ultracool dwarf candidates

Second epoch images of candidate UCDs were taken with the InfraRed Imager and Spectrograph, IRIS2 on the Anglo Australian Telescope (AAT) during service observations on 2006 July 7 and 2006 December 8, with  $J$ -,  $H$ - and  $K_s$ -band filters. The images were reduced using the standard ORACDR package for IRIS2; this included de-biasing, dark subtraction, background subtraction, removal of bad pixels and mosaicing of jittered images.

Spectroscopic observations of one candidate (UCD-1; see Table 2) were also obtained with IRIS2 on the AAT on 2006 September 8. The long slit mode was used with a 1 arcsec slit width in the  $J$ - long and  $H$ - short grisms, covering wavelength ranges  $1.1 - 1.33 \mu\text{m}$  and  $1.46 - 1.81 \mu\text{m}$  with a dispersion of  $0.225 \text{ nm/pixel}$  and  $0.341 \text{ nm/pixel}$ , respectively ( $R \sim 2400$ ). A total exposure time of 20 minutes in

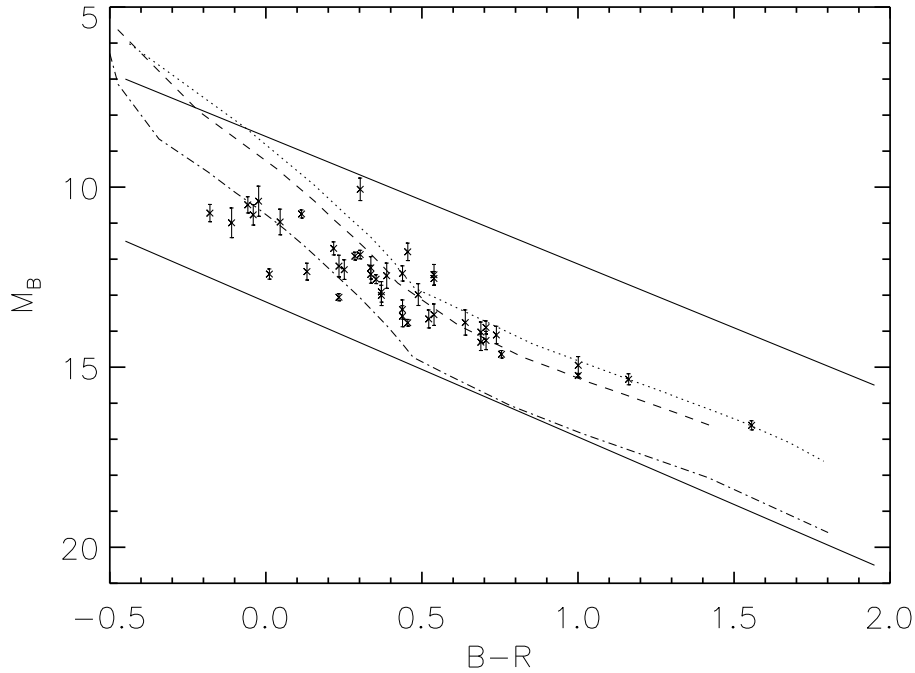


**Figure 2.** WD colour-magnitude diagram for MS99 WDs with known parallax (crosses). Photometry is on the SuperCOSMOS system. Overplotted are model cooling tracks (see main text) for WD masses of  $0.5$ ,  $0.7$  and  $1.2M_{\odot}$  (dotted, dashed and dot-dashed lines respectively). Our WD region in the CMD lies between the two solid lines.

**Table 2.** Candidate UCD-WD binary systems. Coordinates are J2000. Photometry is from 2MASS, SuperCOSMOS and DENIS (where available). The last three columns show which UCD candidates have second epoch imaging (see Section 3.3), which pairs have been confirmed (or not) through common proper motion and which candidates have been confirmed as a UCD or WD with spectroscopy (see Section 4).

Name	RA	Dec	<i>B</i> -	<i>R</i> -	<i>I</i> -	<i>J</i> -	<i>H</i> -	<i>K</i> -	Sep (arcsec)	2nd epoch	CPM	Spec
UCDc-1	00 30 06.26	-37 39 48.2	-	-	18.30	15.2	14.4	13.8	89	IRIS2	Y	Y
WDc-1	00 30 11.90	-37 40 47.2	16.77	16.35	15.97	16.1	15.8	-	-	-	-	Y
UCDc-2	00 56 14.71	-40 36 03.6	-	-	-	15.8	15.0	14.3	922	IRIS2	N	-
WDc-2	00 57 18.72	-40 45 29.6	15.80	15.07	13.67	12.4	-	-	-	-	-	-
UCDc-3	03 02 07.70	-09 41 57.1	-	-	17.66	15.8	15.0	14.5	136	IRIS2	N	-
WDc-3	03 02 03.00	-09 43 54.9	17.63	17.35	17.34	-	-	-	-	-	-	-
UCDc-4	05 20 35.40	-18 54 27.7	-	-	17.64	15.9	15.1	14.7	145	IRIS2	N	-
WDc-4	05 20 40.03	-18 56 37.9	18.34	16.40	17.92	-	-	-	-	-	-	-
UCDc-5	10 12 35.59	-10 51 02.2	-	-	18.13	15.3	14.6	14.1	465	IRIS2	?	-
WDc-5	10 12 43.89	-10 43 33.8	19.48	18.34	17.87	-	-	-	-	-	-	-
UCDc-6	10 40 43.41	-16 48 20.5	-	-	-	15.9	15.2	14.8	124	IRIS2	?	-
WDc-6	10 40 39.17	-16 50 08.3	20.34	19.54	19.12	-	-	-	-	-	-	-
UCDc-7	14 05 37.54	-05 51 53.6	-	-	17.80	15.8	15.2	14.6	164	-	-	-
WDc-7	14 05 44.98	-05 49 51.9	16.66	16.80	16.87	-	-	-	-	-	-	-
UCDc-8	23 21 21.55	-13 26 28.3	-	-	-	14.5	13.5	13.1	73	IRIS2	?	-
WDc-8	23 21 14.38	-13 27 36.8	19.23	18.42	18.00	-	-	-	-	-	-	-

Notes - ? Indicates uncertainty due to a small measured motion and high uncertainties associated with these measurements (see text).

each band was obtained and the target was nodded along the slit in an “ABBA” pattern with individual exposure times of 300s. Standard dome flats and Xenon arcs were taken at the end of the night and an F5V star was observed at a similar airmass to the target to provide telluric correction. The

observing conditions were reasonable with an average seeing of  $0.8 - 1.2$  arcsec.

Standard IRAF routines were used to reduce the spectra including flat fielding and cosmic ray removal. The spectra were extracted with APALL, using a chebyshev function to fit the background and a third order legendre function to trace

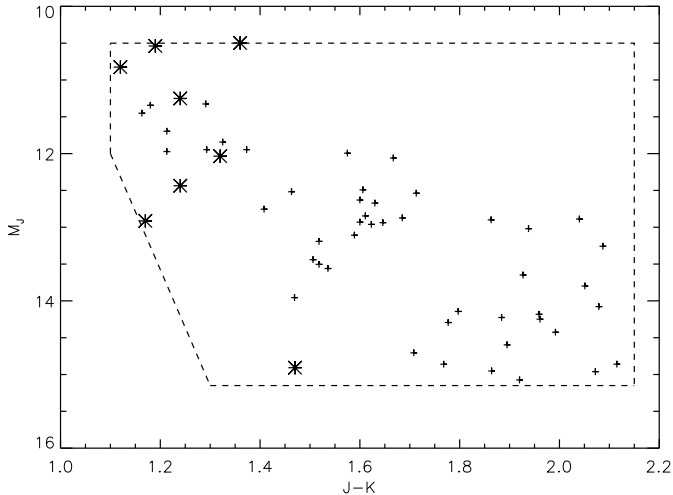


**Figure 3.**  $M_J$  against  $J-K$  colour-magnitude diagram showing the location of the companion UCD candidates (stars) when they are assumed to be at the same distance as their associated WD. Our UCD selection criteria is indicated with a dashed line, and UCDs with known parallax from DWARFARCHIVES.ORG are plotted as plus signs.

the fit to the spectrum. The wavelength calibration was done using the spectrum from a Xenon arc lamp, using IDENTIFY to reference the arc lines and the DISPCOR routine to correct the dispersion of the spectrum. This method was repeated for each of the differenced AB pairs, and the wavelength calibrated spectra were median combined and flux calibrated using the telluric standard and the spectra of a blackbody with a  $T_{\text{eff}} = 7500\text{K}$ . Annotated spectra are shown in Fig. 4 and Fig. 5.

### 3.2 White dwarf candidate

A Spectrum of WDC-1 (2MASSJ0030 – 3740) was obtained with FORS1 on the VLT on 2007 January 24, with directors discretionary time in program 278.C-5024(A), using the longslit mode in the optical wavelength range 3800 – 5200 Å and a dispersion of 50 Å/mm. Three integrations of 600s were taken, giving a total exposure time of 30 minutes. Spectra of a DC WD and a standard F-type star were also taken and used for calibration. Sky flats were taken and HgCd arcs were used for wavelength calibration.

Standard IRAF packages were used to reduce the spectra including debiasing, flat fielding and removal of bad pixels; the three spectra were then extracted and wavelength calibrated as described in Section 3.1. The resulting spectra of both WDC-1 and the standard were divided by the smooth DC WD spectrum, which has no intrinsic spectral features, enabling correction for the instrumental response. The standard star was then used for flux calibration and the final spectrum of 2MASSJ0030 – 3740 is shown in Fig. 6.

### 3.3 Proper motions

The imaging data, as described in Section 3.1 were used to calculate proper motions of our UCD candidates. The IRAF routines GEOMAP and GEOXYTRAN were used to transform between the available multi-epoch images, using an average

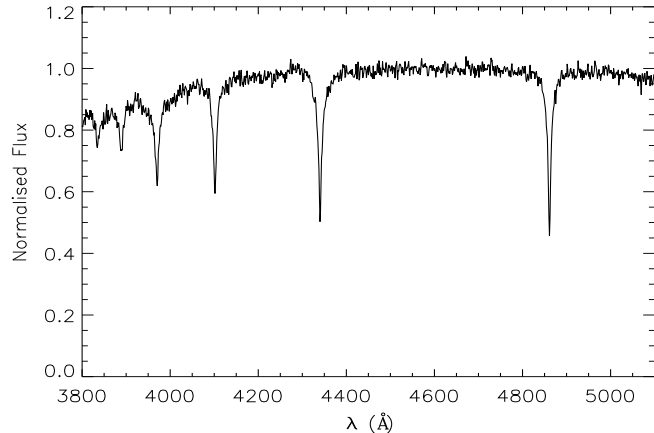


**Figure 6.** Optical spectrum of the confirmed white dwarf WDC-1 (2MASSJ0030 – 3740), flux calibrated and normalised at 4600Å.

of 15 reference stars. In addition a correction was applied to the derived proper motions to account for the average (but small) proper motion of the reference stars. This allowed any motion of the UCD candidates to be accurately measured. Proper motion uncertainties were estimated from centroiding accuracies combined with the residuals associated with our derived transformations.

Amongst the eight candidate binary pairs, three of the UCD candidates were ruled out since they are not common proper motion companions (at  $>3\sigma$ ), three remain uncertain due to the relatively small motion expected between epochs (compared to the uncertainties associated with the inter-epoch transforms) and one remains unobserved (see Table 2 for a summary of these results).

Second epoch IRIS2 measurements of candidate UCDC-1 (2MASS J0030 – 3739) revealed a significant motion over the 6.8 year baseline between the 2MASS first epoch and the IRIS2 second epoch images. The large field of view of IRIS2 ( $7 \times 7$  arcmin) allowed us to measure the proper motion of both the UCD and the WD candidate from the same 2-epoch image set, which clearly revealed the common proper motion. Our final proper motion measurements were based on four individual measurements: pairing up  $J$ -,  $H$ - and  $K$ -band images from the 2MASS and IRIS2 epochs appropriately, as well as pairing up a SuperCOSMOS  $I$ -band as first epoch with the IRIS2  $J$ -band image as second epoch. The last combination is over a relatively longer baseline of 15.86 years, although may suffer from larger chromatic effects due to the different bands. Our final proper motions were an average of these four measurements, and the associated uncertainties were estimated from their standard deviation. Our measured proper motions of the pair are given in Table 5. Multi-band  $BRIJHK$   $2 \times 2$  arcmin finder charts centred on 2MASSJ0030 – 3739 are shown in Fig. 7.

## 4 SPECTRAL CLASSIFICATION

### 4.1 UCDC-1: 2MASSJ0030-3739

#### 4.1.1 Spectral ratios

We estimate a spectral type for 2MASSJ0030 – 3739 based on spectral ratios used in previously published work. Our  $J$ -band spectral coverage is 1.1 – 1.35  $\mu\text{m}$ . In this range we

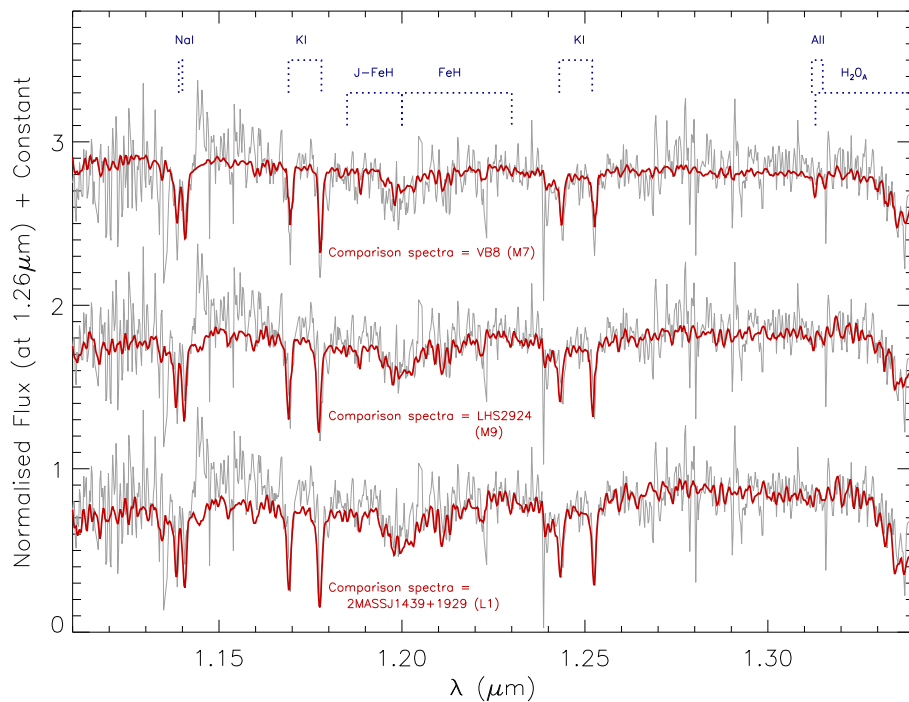


**Figure 4.** *J*-band spectra of 2MASSJ0030 – 3739 (thin grey line), shown with comparison spectra (thick line) of an M7, M9 and L1 type (top to bottom) from Cushing, Rayner & Vacca (2005) overlaid.

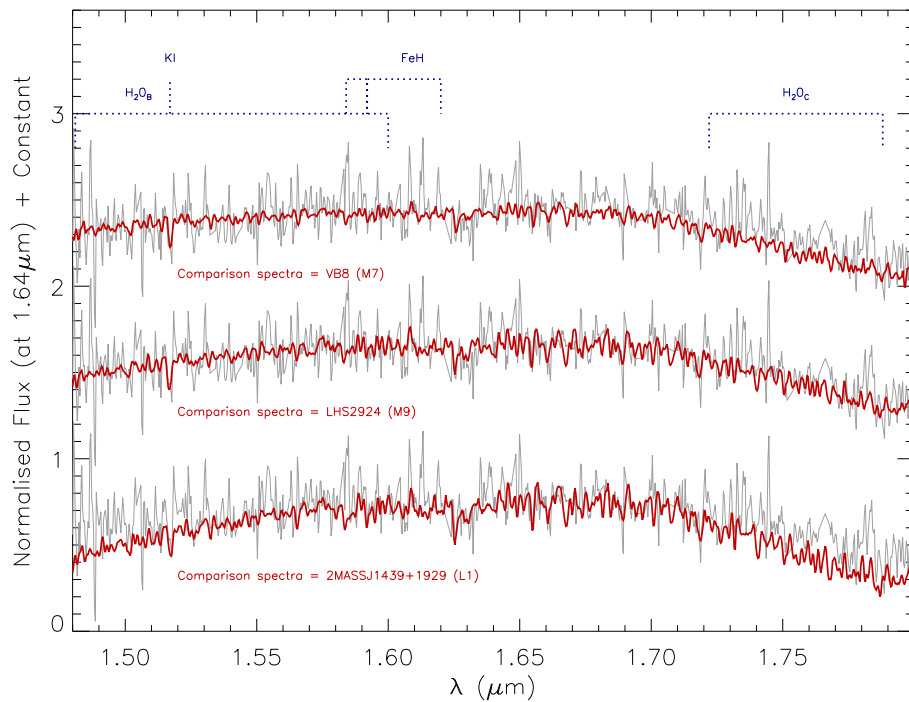


**Figure 5.** *H*-band spectra of 2MASSJ0030 – 3739 (thin grey line). See caption to Fig. 4.

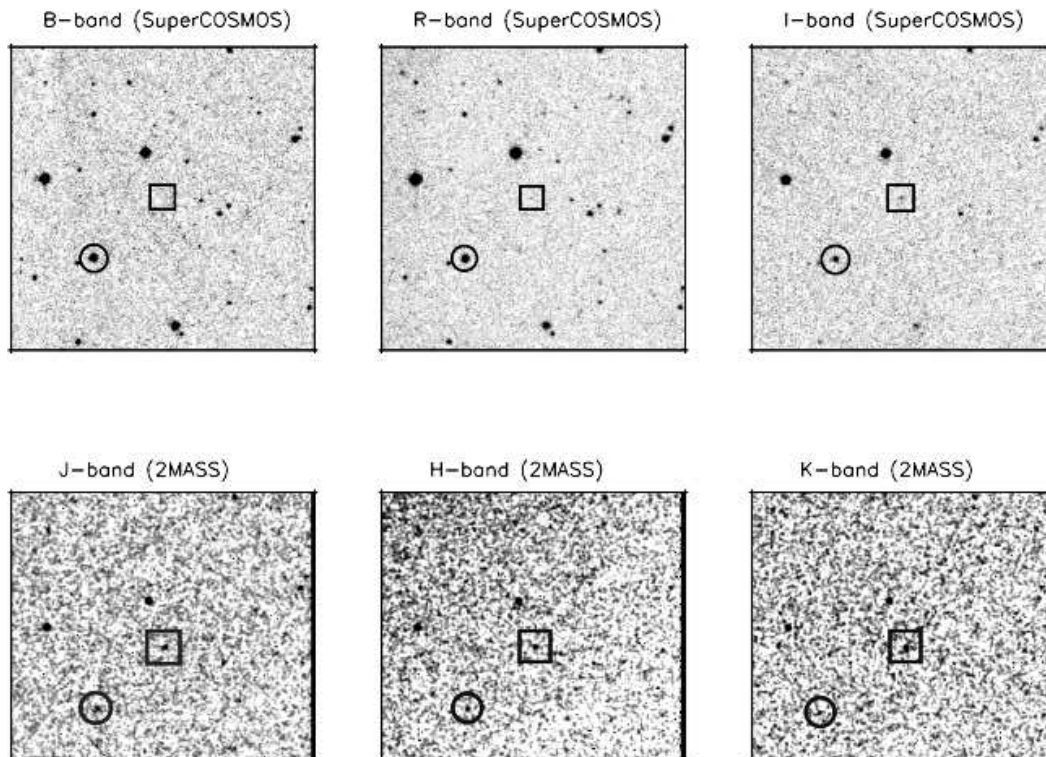


**Figure 7.** SuperCOSMOS and 2MASS images show UCDC-1 (2MASSJ0030 – 3739; squares) and WDc-1 (2MASSJ0030 – 3740; circles).

use the FeH ratio from Slesnick et al. (2004), the  $J$ - FeH and  $H_2O_A$  ratio from McLean et al. (2003). We measure a ratio of 0.854 for FeH, and using the spectral type relation from Slesnick et al. (2004), estimate a spectral type of M9 from this ratio. The  $J$ - FeH ratio of 0.85 combined with the spectral type relations from fig. 12 of McLean et al. (2003) gives a spectral range M8-L3. At the edge of our spectral coverage in the  $J$ - band, when strong water vapour absorption starts to appear, we measure the  $H_2O_A$  ratio as 0.554. The relation between  $H_2O_A$  and spectral type in fig. 11 of McLean et al. (2003) indicates an  $\sim$ L1 type from this ratio.

Our  $H$ - band spectrum covers wavelengths 1.45 – 1.81  $\mu\text{m}$ , for which we used  $H_2O$  ratios from Reid et al. (2001)[ $H_2O_C$ ] and McLean et al. (2003)[ $H_2O_B$ ]. The  $H_2O_C$  ratio of 0.697 indicates an  $L1.5 \pm 2$  and the  $H_2O_B$  ratio of 0.9 is consistent with an M8-M9 type. All the ratios we consider are indicated in Fig. 4 and Fig. 5, and our spectral ratio results are summarised in Table 3.

#### 4.1.2 Comparison to template spectra

Template spectra of known late M and early L dwarfs were used to make a comparison to the overall profile of 2MASSJ0030 – 3739, as well as a comparison to the depth of the absorption in spectral features such as the KI (1.168, 1.179 and 1.243, 1.254  $\mu\text{m}$ ), NaI(1.138, 1.141  $\mu\text{m}$ ) and the AlI (1.311, 1.314  $\mu\text{m}$ ) doublets in the  $J$ - band; and the blended KI doublet (1.517  $\mu\text{m}$ ) and FeH (1.58, 1.59 and 1.62  $\mu\text{m}$ ) in the  $H$ - band. In general alkali metal lines weaken at the M/L boundary (McLean et al. 2000), but

the NaI, AlI, FeH and KI doublets are still clearly recognisable for the purposes of a comparison. The spectra of an M7(VB8), M9(LHS2924) and L1(2MASSJ1439+1929) from Cushing, Rayner & Vacca (2005) were rebinned to the dispersion of our near infrared spectra and normalised at 1.26 and 1.64  $\mu\text{m}$  in the  $J$ - and  $H$ - bands respectively (Fig. 4 and 5). Visual inspection of the blended line features reveal the spectra are most consistent with an  $\sim$ M9 type.

#### 4.1.3 Equivalent widths

We calculated equivalent widths for the four neutral alkali (KI) lines present in the  $J$ - band spectra using the methods of McLean et al. (2003). An IDL program was used to interactively determine the equivalent width of each KI line, which were compared with those of McLean et al. (2003), to estimate a spectral type for each line (see their table 7). In order to reduce the amount of bias when selecting the reference continuum, the process was repeated 12 times using a continuum measured at different relative positions (within 0.05  $\text{\AA}$  from the centre of the line) and the mean of the measurements used. A width of 4.89  $\text{\AA}$  at the 1.168  $\mu\text{m}$  line indicates an M8/9; while the other three KI line widths at 1.177, 1.243 and 1.254  $\mu\text{m}$  are all consistent with an M7/8 type.

Analysis of the spectra of 2MASSJ0030 – 3739, through the use of spectral ratios, comparison to template spectra and equivalent widths (summarised in Table 3) are all consistent with a spectral type  $M9 \pm 1$ . We can use the relation between spectral type and absolute magnitude from Dahn et al. (2002) to calculate a range in  $M_J$  of 10.85 – 12.04 for the spectral range M8-L0. Thus, combining this with

**Table 3.** Estimated spectral types for 2MASSJ0030 – 3739.

Method	Reference	Spectral type
Ratio FeH (1.200/1.230 $\mu\text{m}$ )	Slesnick ('04)	M9
" <i>J</i> - FeH (1.185/1.200 $\mu\text{m}$ )	McLean ('03)	M8-L3
" $\text{H}_2\text{O}_A$ (1.313/1.343 $\mu\text{m}$ )	"	$\sim\text{L1}$
" $\text{H}_2\text{O}_C$ (1.722/1.788 $\mu\text{m}$ )	Reid ('01)	$\text{L1.5} \pm 2$
" $\text{H}_2\text{O}_B$ (1.480/1.600 $\mu\text{m}$ )	"	M8-M9
SC <i>J</i> -	...	$\text{M9} \pm 1$
SC <i>H</i> -	...	$\text{M9} \pm 1$
EW KI (@ 1.168 $\mu\text{m}$ )	McLean ('03)	M8-M9
EW KI (@ 1.177 $\mu\text{m}$ )	"	M7-M8
EW KI (@ 1.243 $\mu\text{m}$ )	"	M7-M8
EW KI (@ 1.254 $\mu\text{m}$ )	"	M7-M8

Notes: SC- Spectral Comparison, EW- Equivalent Width.

the measured *J*- band magnitude from 2MASS, we estimate 2MASSJ0030 – 3739 is at a distance of 41 – 75 pc.

#### 4.2 WDc-1: 2MASSJ0030-3740

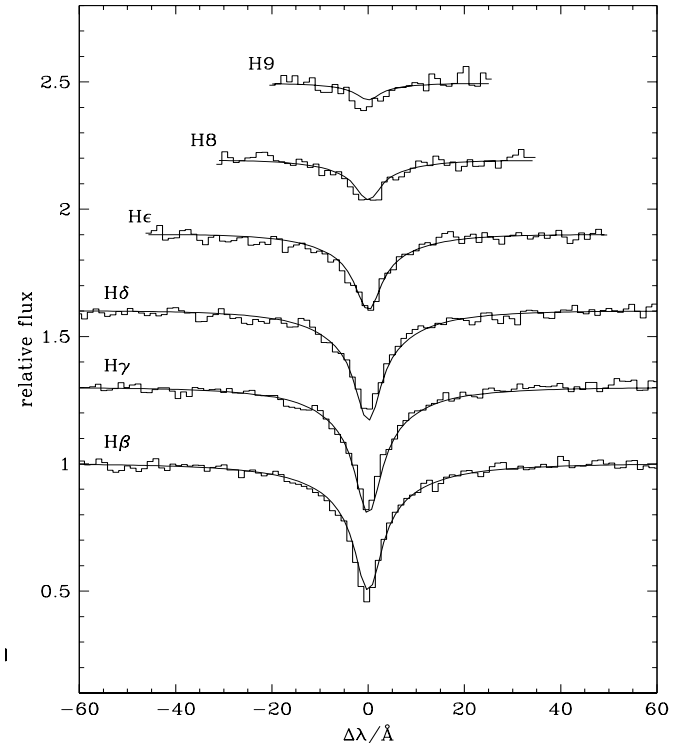
We derived WD parameters,  $T_{\text{eff}}$  and  $\log(g)$  from a fit of the Balmer lines using the fitting routine FITPROF described in Napiwotzki, Green & Saffer (1999). The WD spectrum is modelled using an extensive grid of spectra computed with the model atmosphere code of Detlev Koester described in Finley, Koester & Basri (1997). Observational and theoretical Balmer line profiles are normalised to a linear continuum and the atmospheric parameters determined with a  $\chi^2$  algorithm. Our best fit is shown in Fig. 8. Results are  $T_{\text{eff}} = 7600 \pm 20$  K and  $\log(g) = 8.09 \pm 0.04$  (formal errors from the fit routine to one sigma).

Realistic error estimates are often substantially larger than the formal statistical estimates. Napiwotzki et al. (1999) derived a relative uncertainty of 2.3 per cent in  $T_{\text{eff}}$  and 0.075 dex in  $\log(g)$  from a sample of DA WDs analysed using the same fitting method. We adopt this temperature uncertainty for our following estimates, but the gravity determination is likely subject to a systematic overestimate. The mass distribution of WDs peaks close to  $0.6 M_{\odot}$  (e.g. Napiwotzki et al. 1999; Bergeron, Gianninas & Bourdreaud 2007), corresponding to  $\log(g)$  values close to 8.0. Spectroscopic investigations applying the method explained above show a trend of the  $\log(g)$  distribution peaking at increasingly higher values for decreasing temperatures (Bergeron et al. 2007). This trend starts at 11500 K putting the white dwarf analysed here in the affected region. Taken at face value, this would indicate on average higher masses for cool WDs. However, as argued by Bergeron et al. (2007) and Engelbrecht & Koester (2007) this can be ruled out. A source of extra line broadening must be present in these stars. However, the exact nature of this mechanism is still under discussion and as pointed out in Bergeron et al. (2007) anecdotal evidence suggests that some stars are affected and others are not.

Here we take a pragmatic approach. We used a large sample of DA white dwarfs observed in the course of the SPY programme (Napiwotzki et al. 2001) to derive an empirical correction. Spectra of these stars were analysed using the same model grid and very similar analysis methods as the WD discussed here. We estimated a shift of the  $\log(g)$

**Table 4.** Fit results and derived quantities of WD mass, cooling age and absolute brightness for the corrected and uncorrected case discussed in Section 4.2.

	$T_{\text{eff}}$ [K]	$\log(g)$ [ $\text{cm s}^{-2}$ ]	M [ $M_{\odot}$ ]	$t_{\text{cool}}$ [Gyr]	$M_V$
solution 1	7600	8.09	0.65	1.48	13.4
solution 2	7600	7.79	0.48	0.94	12.9

**Figure 8.** Model atmosphere fit of the Balmer lines of 2MASSJ0030 – 3740 with our best fit parameters  $T_{\text{eff}} = 7600$  K and  $\log(g) = 7.79$ . Observed and theoretical fluxes were normalised to the continuum. Line profiles are shifted for clarity.

distribution caused by this unknown mechanisms of 0.3 dex in the  $T_{\text{eff}} = 7500 - 8000$  K range. The corrected gravity is then  $\log(g) = 7.79$ . As mentioned above it is not entirely clear whether all cool WDs are affected. Thus we will use the corrected and uncorrected gravity values for further discussion. WD masses and cooling ages were calculated by interpolation in the Benvenuto & Althaus (1999) cooling tracks for white dwarfs with thick hydrogen envelopes. Results are listed in Table 4.

We used the latest table of DA colours from Holberg & Bergeron (2006) combined with the model  $M_V$  values from Table 4, to calculate a range in  $M_I$  for  $T_{\text{eff}}$  ( $7600 \pm 175$  K) and  $\log(g)$  estimates. Combined with the well calibrated *I*- band magnitude from DENIS we determined a distance for 2MASSJ0030 – 3740 of 27 – 59 pc, which is consistent with our distance estimate for the UCD companion 2MASSJ0030 – 3739. We thus suggest our binary is at a distance of 41 – 59 pc, which gives a binary separation of 3650 – 5250 AU.

## 5 DISCUSSION

### 5.1 A randomly aligned pair?

In order to determine if the new system is a bonafide UCD-WD binary, we have statistically assessed the likelihood that two such objects could be a line-of-sight association with photometry and proper motion consistent with binarity by random chance. To do this we began with the UCD luminosity function of Cruz et al. (2007), which gives a number density of  $(4.9 \pm 0.6) \times 10^{-3}$  UCDs per  $\text{pc}^{-3}$ . We then calculated a volume associated with 1532 circular areas on the sky (one for each of our WD candidate sample), with radii of 89 arcsec (separation of the components) and a line-of-sight depth of  $58 \pm 17 \text{pc}$  (approximate distance to the new M9 UCD, using relations from Dahn et al. 2002). This volume equates to  $58 \pm 26 \text{pc}^{-3}$ , giving a total expected number of 0.28 UCDs to be within 89 arcsec of one of our WD candidates.

To factor in the probability that two objects might have a common proper motion at the level as our measurements, we downloaded a magnitude-limited sample ( $R < 20$ ) from the SuperCOSMOS Science Archive, applying the same minimum proper motion requirement that was used to create our WD candidate sample. This sample of 160 sources was centred on our WD and selected from a large circular sky area of radius 90 arcmin. We then constructed a proper motion vector-point-diagram, and counted sources that were found to be within the  $2\sigma$  uncertainty circle of the measured UCD proper motion. We found that four of the 160 sources had proper motion consistent with our UCD, suggesting a probability of  $2.4 \pm 1.2$  per cent that such common proper motion could occur by random chance (where we assume Poisson uncertainties associated with this and other samples considered in this discussion).

An additional requirement fulfilled by our UCD-WD system is that the colour-magnitude information must be consistent with a common distance (see Fig. 3), and we found that 53 per cent ( $786 \pm 28$ ) of our WD candidate sample were photometrically consistent with being at the same distance as the UCD.

Finally we consider what fraction of our WD candidates might be spurious, and thus not able to contribute to non binary line-of-sight associations where the WD has been confirmed spectroscopically. In the magnitude range  $R < 14$ , where MS99 is thought to be essentially complete, we find that 66 per cent of our WD candidates are included in the MS99 catalogue. This suggests that, at least for brighter magnitudes, our WD candidates are relatively free from contaminating objects, and that our selection techniques are robust. While we cannot be sure that the same low-level of contamination applies to the full magnitude range, we take the conservative approach and consider the full WD candidate sample as potentially contributing to non-binaries that appear to be UCD-WD pairs.

Taking into account all these factors, we estimate that we would expect  $0.0036 \pm 0.0025$  randomly aligned UCD-WD pairs with  $\leq 89$  arcsec separation and proper motion and photometry consistent with binarity at the level of our observations. The likelihood of the system being merely a line-of-sight association is thus vanishingly small, and we can assume that the UCD-WD pair is a gravitationally bound binary system.

### 5.2 Binary age

The age of the binary system can be constrained from the white dwarf mass and cooling age. For our corrected fit, we suggest that 2MASSJ0030 – 3740 is  $0.48 M_{\odot}$  and has a cooling age of 0.94 Gyr. We access the IFMR determinations of Weidemann (2000), Dobbie et al. (2004), Dobbie et al. (2006), Ferrario et al. (2005), Catalán et al. (2008) and Kalirai et al. (2008) to estimate a likely, initial-mass constraint for the main-sequence progenitor star of  $1 - 2 M_{\odot}$ . The main sequence lifetime of a progenitor of this mass is likely  $> 1 \text{Gyrs}$  (probably several Gyrs) and thus is not useful when trying to constrain the upper age limit of the system. Thus the upper age limit of our system remains uncertain. Note that if the WD mass were higher, for example if the helium enrichment of the atmosphere is lower than typical (see Section 4.2) then the WD’s  $\log(g)$  could be as high as 8.1 dex, with a WD mass of  $\sim 0.65 M_{\odot}$  and cooling age of  $\sim 1.5 \text{Gyrs}$ . This would allow progenitor mass to be constrained to a likely range of  $< 2.7 M_{\odot}$ , giving a main-sequence progenitor lifetime of  $< 0.83 \text{Gyrs}$  (Monteiro et al. 2006), yielding a binary age constraint of 1.5–2.3 Gyrs. This possibility is instructive at least, in demonstrating the level of age constraints (with accompanying UCD constraints) that may be placed on benchmark binaries of this type. However, it is not possible to judge the helium content of the WD’s atmosphere (if any), and we can only confidently place a lower limit on the age of this binary from our best fit cooling age for the WD and the likely length of the main sequence lifetime of the progenitor, which is likely equal to or larger than the white dwarf cooling age. The age of the binary is thus  $> 1.94 \text{Gyrs}$ .

### 5.3 UCD properties

We have estimated  $T_{\text{eff}}$ , mass and  $\log(g)$  from the Lyon group dusty models (Chabrier et al. 2000; Baraffe et al. 2002), using the minimum age of the system (0.94 Gyrs) and our estimated  $M_J$  of 2MASSJ0030 – 3739. The models indicate that 2MASSJ0030 – 3739 has  $T_{\text{eff}} = 2000 - 2400 \text{K}$ ,  $\text{mass} = 0.07 - 0.08 M_{\odot}$  and  $\log(g) = 5.30 - 5.35$ , placing it close to the limit for hydrogen burning. Note that our  $T_{\text{eff}}$  is consistent with the semi-empirical estimates of Golimowski et al. (2004) for an  $M9 \pm 1$  dwarf, which use well measured luminosities and a model constraint on radius (which changes by  $< 10$  per cent for ages of 1 – 5 Gyrs), to determine  $T_{\text{eff}}$  values spanning a wide range of spectral type. The full list of properties for the binary are listed in Table 5.

## 6 FUTURE WORK

A parallax measured distance would allow the luminosity of 2MASSJ0030 – 3739 to be directly measured. Our age constraint would then facilitate a tight model constraint on the radius, and thus an accurate determination of  $T_{\text{eff}}$  and  $\log(g)$ . This UCD could then have a very useful role as part of a testbed for our understanding of ultracool atmospheres. For example, McGovern et al. (2004) studied a set of M dwarfs with young and intermediate ages, and showed that a variety of spectral lines including the  $J$ - band KI

**Table 5.** Parameters of the binary and its components.

Parameter	Value
Separation on sky	89 arcsec
Estimated distance	41 – 59 pc
Estimated line-of-sight separation	3650 – 5250 AU
Minimum age of system	> 1.94 Gyrs
<u>Ultracool Dwarf</u>	
RA	00 30 06.26
DEC	-37 39 48.2
2MASS designation	2MASSJ0030 – 3739
Distance	41 – 75pc
2MASS <i>J</i>	15.2 ± 0.05
2MASS <i>H</i>	14.4 ± 0.05
2MASS <i>K<sub>s</sub></i>	13.8 ± 0.06
DENNIS <i>I</i>	18.4 ± 0.23
DENNIS <i>J</i>	15.06 ± 0.14
SuperCOSMOS <i>I</i>	~18.3
$\mu$ RA	-130 ± 30 mas yr <sup>-1</sup>
$\mu$ DEC	-70 ± 20 mas yr <sup>-1</sup>
Spectral Type	M9 ± 1
Mass	0.07 – 0.08 M <sub>☉</sub>
$T_{\text{eff}}$	2000 – 2400 K
log( <i>g</i> )	5.30 – 5.35 dex
<u>White Dwarf</u>	
RA	00 30 11.9
DEC	-37 40 47.2
2MASS designation	2MASSJ0030 – 3740
Distance	27 – 59 pc
2MASS <i>J</i>	16.1 ± 0.11
2MASS <i>H</i>	15.8 ± 0.15
DENNIS <i>I</i>	16.2 ± 0.07
DENNIS <i>J</i>	15.9 ± 0.22
SuperCOSMOS <i>B</i>	~16.77
SuperCOSMOS <i>R</i>	~16.35
SuperCOSMOS <i>I</i>	~15.97
$\mu$ RA	-83 ± 30 mas yr <sup>-1</sup>
$\mu$ DEC	-70 ± 12 mas yr <sup>-1</sup>
Spectral Type	DA
$T_{\text{eff}}$	7600 ± 175 K
log( <i>g</i> )	7.79 – 8.09 dex
Mass	0.48 – 0.65 M <sub>☉</sub>
WD cooling age	0.94 – 1.5 Gyrs
WD progenitor age	> 1 Gyr

lines, are gravity sensitive. It is also clear that the effects of dust in very late M dwarf atmospheres are not well understood (e.g. Jones et al. 2005). Removing degeneracies in the physical properties of such objects will allow for a more focused testing of available models in this region of  $T_{\text{eff}} - \log(g)$  space.

A more expansive search for benchmark UCD-WD binary systems can be made using the combination of UKIDSS and SDSS (e.g. Day-Jones et al. 2007). These surveys probe a significantly larger volume for UCDs and WDs than 2MASS and SuperCOSMOS, and will thus yield a larger number of wide benchmark binaries, with a broader range of properties. It is likely that significant numbers of binary systems could be identified containing an L/T dwarf and a WD (see Pinfield et al. 2006). Also, if the frequency of wide UCD companions to higher mass stars is of a simi-

lar level to those found around solar type stars, there could be numerous detectable systems with high mass WD components. Tight constraints on binary age will be particularly important when determining the properties of cooler, lower mass UCD companions, since sub-stellar brown dwarfs cool continuously, and their mass and surface gravity depend strongly on age. The broad band spectral morphology of L and T dwarf populations show a significant scatter independent of spectral type, presumably due to variations in surface gravity and metallicity. Thus, the physical constraints offered by benchmark systems of this type could hold great potential to reveal trends linking such spectral changes to variations in UCD physical properties.

## ACKNOWLEDGMENTS

We acknowledge Science and technology Facilities Council (STFC) for their support to ACD, BB, SLF, DJW and JRC, we would also like to acknowledge the helpful advice given from Detlev Koester in this work. This publication has made use of the NASA/IPAC Infrared Science Archive, which is operated by the Jet Propulsion Laboratory, California Institute of Technology, under contract with the National Aeronautics and Space Administration. We have also made use of the data obtained from the SuperCOSMOS Science Archive, prepared and hosted by the Wide Field Astronomy Unit, Institute for Astronomy, University of Edinburgh, which is funded by the STFC. We gratefully acknowledge the UK and Australian government support of the Anglo-Australian Telescope through their STFC and DETYA funding as well as NASA grant NAG5-8299 & NSF grants AST95-20443 and AST-9988087 and Sun Microsystems. We would also like to acknowledge the DENIS project, that has been partly funded by the SCIENCE and the HCM plans of the European Commission under grants CT920791 and CT940627. It is supported by INSU, MEN and CNRS in France, by the State of Baden-Württemberg in Germany, by DGICYT in Spain, by CNR in Italy, by FFwFBWF in Austria, by FAPESP in Brazil, by OTKA grants F-4239 and F-013990 in Hungary, and by the ESO C&EE grant A-04-046. Jean Claude renault from the IAP was the project manager. Observations were carried out thanks to the contribution of numerous students and young scientists from all involved institutions, under the supervision of P. Fouqué, survey astronomer resident in Chile.

## REFERENCES

- Allard F., Hauschildt P.H., Alexander D.R., Tamanai A., Schweitzer A., 2001, ApJ, 556,357  
 Baraffe I., Chabrier G., Allard F., Hauschildt P.H., 2002, A&A, 382, 563  
 Benvenuto O.G., Althaus L.G., 1999, MNRAS 303, 30  
 Bergeron P., Gianninas A., Boudreault S., 2007, in ASP Conf. Ser. 372,15th European Workshop on White Dwarfs, eds. R.Napiwotzki & M.R.Burleigh, (San Francisco: ASP), 29  
 Bessell M.S., 1986, PASP, 98, 1303  
 Burgasser A.J., Geballe T.R., Leggett S.K., Kirkpatrick J.D., Golimowski D.A., 2006, ApJ, 637, 1067

- Burgasser A.J., Burrows A., Kirkpatrick J.D., 2006, *ApJ*, 639,1095
- Burleigh M.R., Clarke F.J., Hodgkin S.T., 2002, *MNRAS*, 331, 41
- Burleigh M.R., Hogan E., Dobbie P.D., Napiwotzki R., Maxted P.F.L., 2006, *MNRAS*, 373, L55
- Burleigh M.R., Marsh T.R., Gänsicke B.T., Goad M.R., Dhillon V.S., Littlefair S.P., Wells M., Bannister N.P., Hurkett C.P., Martindale A., Dobbie P.D., Casewell S.L., Baker D.E.A., Duke J., Farihi J., Irwin M.J., Hewett P.C., Roche P., Lewis F., 2006, *MNRAS*, 373, 1416
- Burrows A., Sudarsky D., Hubeny I., 2006, *ApJ*, 640,1063
- Catalán S., Isern J., García-Berro E., Ribas I., Allende Prieto C., Bonanos A.Z., 2008, *A&A*, 477, 213
- Cavanagh B., Hirst P., Jenness T., Economou F., Currie M.J., Todd S., Ryder S.D., 2003, *ASPC*, 295,237
- Chabrier G., Baraffe I., Allard F., Hauschildt P., 2000, *ApJ*, 542, 464
- Chabrier G., Bassard P., Fontaine G., Saumon D., 2000, *ApJ*, 543, 216
- Cruz K.L., Reid I.N., Liebert J., Kirkpatrick J.D., Lowrance P.J., 2003, *AJ*, 126, 2421
- Cruz K.L., et al., 2007, *ApJ*, 133, 439
- Cushing M.C., Rayner J.T., Vacca W.D., 2005, *ApJ*, 623, 1115
- Dahn C.C., et al., 2002, *AJ*, 124, 1170
- Day-Jones A.C., Pinfield D.J., Napiwotzki R., Burningham B., Jones H.R.A., Jenkins J.S., 2007, *AAS*, 221, 16204
- Delorme P., Delfosse X., Albert, L., Artigau E., Forveille T., Reylé C., Allard F., Homeier D., Robin A., Willott C.J., Liu M., Dupuy T., 2008, arXiv0802.4387D
- Dobbie P.D., Pinfield D.J., Napiwotzki R., Hambly N.C., Burleigh M.R., Barstow M.A., Jameson R.F., Hubeny I., 2004, *MNRAS*, 355,39
- Dobbie P.D., Burleigh M.R., Levan A.J., Barstow M.A., Napiwotzki R., Holberg J.B., Hubeny I., Howell S.B., 2005, *MNRAS*, 357, 1049
- Dobbie P.D., Napiwotzki R., Burleigh M.R., Barstow M.A., Boyce D.D., Casewell S.L., Jameson R.F., Hubeny I., Fontaine G., 2006, *MNRAS*, 369, 383
- Engelbrecht A., Koester D.2007, in *ASP Conf. Ser.* 372, 15th European Workshop on White Dwarfs, eds. R.Napiwotzki & M.R.Burleigh, (San Francisco: ASP), 289
- Farihi J., Christopher M., 2004, *AJ*, 128, 1868
- Farihi J., Becklin E.E., Zuckerman B., 2005, *AJ*, 161, 394
- Farihi J., Hoard D.W., Wachter S., 2006, *ApJ*, 646, 480
- Farihi J., Burleigh M.R., Hoard D.W., 2008, *ApJ*, 674, 421
- Farihi J., Becklin E.E., Zuckerman B., 2008, arXiv:0804.0237
- Ferrario L., Wickramasinghe D., Liebert J., Williams K.A., 2005, *MNRAS*, 361, 1131
- Finley D.S., Koester D., Basri G.1997, *ApJ* 488, 375
- Folkes S.L., Pinfield D.J., Kendall T.R., Jones H.R.A., 2007, *MNRAS*, 378,901
- Geballe T.R., Knapp G.R., Leggett S.K., Fan X., Golimowski D.A., 2003, *csss*, 12,670
- Gizis J.E., Kirkpatrick J.D., Burgasser A., Reid I.N., Monet D.G., Liebert J., Wilson J.C., 2001, *ApJ*, 551, 163
- Golimowski D.A., et al., 2004, *AJ*, 127, 3516
- Holberg J.B., Oswalt T.D., Sion E.M, 2002, *ApJ*, 571, 512
- Holberg J.B., Bergeron P., 2006, *AJ*, 132, 1221
- Howell S.B., Ciardi D.R., 2001, *ApJ*, 550, 57
- Jeans J.H., 1924, *MNRAS*, 85, 2
- Jones H.R.A., Steele I.A., 2001, *Bolin Heidelberg Springer*
- Jones H.R.A., Pavlenko Y., Viti S., Barber R.J., Yakovina L.A., Pinfield D., Tennyson J., 2005, *MNRAS*, 358, 105
- Kalirai J.S., Hansen B.M.S., Kelson D.D., Reitzel D.B., Rich R.M., Richer H.B., 2008, *ApJ*, 676, 594
- Kilkenny D., Heber U., Drilling J.S., 1988, *AAOC*, 12, 1
- Kleinman S.J., et al., 2004, *ApJ*, 607, 426
- Knapp G.R., et al., 2004, *AJ*, 127, 3553
- Knox R.A., Hawkins M.R.S., Hambley N.C., 1999, *MNRAS*, 306, 736
- Leggett S.K., 1992, *ApJ*, 82, 351
- Littlefair S.P., Dhillon V.S., Marsh T.R., Gänsicke B.T., Southworth J., Watson C.A., 2006, *Sci*, 314, 1578
- Liu M.C., Leggett S.K., Chiu K., 2007, 660, 1507
- Maxted P.F.L., Napiwotzki R., Dobbie P.D., Burleigh M.R., 2006, *NAT*, 442, 543
- McCook G.P., Sion E.M., 1999, *ApJS*, 121
- McGovern M.R., McLean I.S., Kirkpatrick J.D., Burgasser A.J., Prato L., 2004, *AAS*, 20513510
- McLean I.S., et al., 2000, *ApJ*, 533, 45
- McLean I.S., McGovern M.R., Burgasser A.J., Kirkpatrick J.D., Prato L., Kim S.S., 2003, *ApJ*, 596, 561
- Metchev S.A., Hillenbrand L.A., 2006, *ApJ*, 651, 1166
- Monet D.G., Dahn C.C., Vrba F.J., Harris H.C., Pier J.R., Luginbuhl C.B., Ables H.D., 1992, *AJ*, 103,638
- Monteiro H., Jao W.C., Henry T., Subasavage J., Beaulieu T., 2006, *ApJ*, 638, 446
- Mullally F., Kilic M., Reach W.T., Kuchner M.J., von Hippel T., Burrows A., Winget D.E., *ApJS*, 171, 206
- Nakajima T., Oppenheimer B.R., Kulkarni S.R., Golimowski D.A., Matthews K., Durrance S.T., 1995, *Nat*, 378, 463
- Napiwotzki R., Green P.J., Saffer R.A., 1999, *ApJ* 517, 399
- Napiwotzki R., et al., 2001, *AN*, 322, 411
- Natali F., Natali G., Pompei E., Pedichini F., 1994, *A&A*, 289, 756
- Padoan P., Nordlund 2002, *ApJ*, 576,870
- Panei J.A., Althaus L.G., Benvenuto O.G., 2000, *A&A*, 353, 970
- Pinfield D.J., Jones H.R.A., Lucas P.W., Kendall T.R., Folkes S.L., Day-Jones A.C., Chappelle R.J., Steele I.A., 2006, *MNRAS*, 368,1281
- Rebolo R., Zapatero-Osorio M.R., Martin E.L., 1995, *Nat*,377,129
- Reid I.N., Burgasser A., J., Cruz K.L., Kirkpatrick J.D., Gizis J.L., 2001, *AJ*, 121, 1710
- Reipurth B., Clarke C., 2001, *AJ*, 122, 432
- Rice W.K.M., Armitage P.J., Bonnell I.A., Bate M.R., Jeffers S.V., Vine S.G., 2003, *MNRAS*, 346,36
- Saumon D., et al., 2007, *ApJ*, 656,1136
- Scholz R.D., Lodieu N., Ibata R., Bienaymé O., Irwin M., McCaughrean M.J., Schwöpe A., 2004, *MNRAS*, 347, 685
- Schröder K.P., Pauli E.M., Napiwotzki R., 2004, *MNRAS*, 354, 727
- Silvestri N.M., Hawley S.L., Oswalt T.D., 2005, *AJ*, 129, 2428
- Slesnick C.L., Hillenbrand L.A., Carpenter J.M., 2004, *ApJ*, 610, 1045
- Smith J.A., Tucker D.L., Allam S.S., Jorgensen A.M., 2002, *AAS*, 20110408
- Stark M.A., Wade R.A., 2003, *AJ*, 126,1455

- Steele P.R., Burleigh M.R., Dobbie P.D., Barstow M.A.,  
2007, MNRAS, tmp, 1021  
Warren S.J., et al., 2007, MNRAS, 381, 1400  
Weidemann V., 2000, A&A, 363, 647  
Wesemael F., van-Horn H.M., Savedoff M.P., Auer L.H.,  
1980, ApJ, 43, 159  
Whitworth A.P., Goodwin S.P., 2005, AN, 326, 899  
Williams K.A., Bolte M., Koester D., 2004, ApJ, 615, 49  
Yong D., Lambert D.L., 2003, PASP, 115, 22  
Zuckerman B., Becklin E.E., 1992, ApJ, 386, 260

This paper has been typeset from a  $\text{\TeX}$ / $\text{\LaTeX}$  file prepared  
by the author.